

Exact computations of the acoustic radiation force on a sphere using the translational addition theorem

Glauber T. Silva, *Member, IEEE*, André L. Baggio, J. Henrique Lopes, and Farid G. Mitri, *Member, IEEE*

Abstract—In this paper, the translational addition theorem for spherical functions is employed to exactly calculate the acoustic radiation force produced by an arbitrary shaped beam on a sphere suspended in an inviscid fluid. The radiation force is given in terms of the beam-shape and the scattering coefficients. Each beam-shape coefficient (BSC) is the complex weight of a multipole mode in partial-wave expansion of the incident beam. Moreover, they depend on the choice of the reference frame which is defined by the sphere's center. On the other hand, the scattering coefficients are obtained from the acoustic boundary conditions across the sphere's surface. Given a set of known BSCs, the translational addition theorem can be used to obtain the new coefficients relative to the sphere's position. Such approach is particularly useful when no closed-form expression of the incident pressure is known, but its BSCs are available. This is the case of a spherically focused ultrasound beam, for which we compute the radiation force on an absorbing compressible sphere arbitrarily placed in the fluid. The analysis is carried out in the Rayleigh and the resonant scattering regimes. It is shown that the focused beam may trap a spherical particle in the Rayleigh scattering regime.

Index Terms—Acoustic Radiation Force, Translational Addition Theorem, Single-beam Acoustical Tweezer.

I. INTRODUCTION

An increasing interest on ultrasound radiation force has been triggered after the concept of acoustical tweezers was introduced by Wu [1]. In acoustophoresis, the radiation force of a ultrasound standing wave is used in contactless manipulation, separation, and trapping of small particles and cells [2]. Two-dimensional tweezers are achieved in lab-on-a-chip devices [3] and by employing circular phased-arrays [4]. Single-beam acoustical

tweezer has also been developed by using a tightly focused beam [5].

The acoustic radiation force exerted by a plane or a spherical wave on a suspended sphere in a nonviscous fluid has been extensively investigated over the last century [6], [7], [8], [9], [10], [11], [12]. Based on the partial-wave expansion of the incident and the scattered waves, the axial radiation force exerted on a sphere by a planar piston beam [13], [14], a spherically focused beam [15], Bessel beams [16], [17], [18], [19], and a Gaussian [20] beam. In all these studies, the sphere is located in the axis of the beam. For focused beams, the analysis was restricted to the sphere placed in the focus point.

The design of single-beam acoustical tweezers requires an analysis of how radiation force on the sphere behaves in the vicinity of the transducer's focus point. So far, this analysis has been only performed for the geometric scattering regime [21], for which $ka \gg 1$, where k is the incident wavenumber and a is the sphere's radius. For other limits such as the Rayleigh ($ka \ll 1$) and the resonant ($ka \sim 1$) scattering regimes, the radiation force can be computed using the partial-wave expansion method [22]. In this method, the radiation force exerted on a suspended sphere is expressed in terms of the beam-shape and the scattering coefficients [23]. Each beam-shape coefficient (BSC) is the complex amplitude of an incident partial-wave, while the scattering coefficients are obtained from the acoustic boundary conditions across the sphere's surface. The BSCs carry information regarding to the geometry of the incident beam. Similarly, the scattering coefficients is related to the mechanical properties of the scatter.

The radiation force produced by a spherically focused transducer on a sphere arbitrarily located in the host medium can be obtained by calculating the BSC with respect to the particle's position. Numerical schemes to compute the BSC include the midpoint integral rule [23], [24] and the discrete spherical harmonics transform (DSHT) [25], [26], which is based on the discrete Fourier transform. A description of other quadrature methods to compute BSCs in the context of optical scattering

Glauber T. Silva, André L. Baggio, and J. Henrique Lopes are with Physical Acoustics Group, Instituto de Física, Universidade Federal de Alagoas, Maceió, AL 57072-900, Brazil. Email: glauber@pq.cnpq.br (see <http://www.if.ufal.br/~gaf>)

Farid G. Mitri is with Los Alamos National Laboratory, Materials Physics and Applications Division, MPA-11, Sensors & Electrochemical Devices, Acoustics & Sensors Technology Team, MS D429, Los Alamos, NM, USA 87545.

is provided in Ref. [27]. Both methods require that the incident pressure amplitude should be sampled over a virtual sphere which encloses the beam propagation region, which contains the spherical target. For highly oscillating functions, the midpoint rule requires a large number of sampling points to ensure proper convergence of the BSC computation. Yet the DSHT renders more accurate results with less sampling points, it may develop numerical errors related to aliasing due to undersampling and spectral leakage caused by function domain truncation.

In order to circumvent numerical approximations, we propose a method to exactly calculate the acoustic radiation force based on the partial-wave expansion method [22], [26] and the translational addition theorem [28]. A similar method has been devised to calculate the radiation pressure generated by an electromagnetic wave [29]. The proposed method is used to calculate the radiation force produced by a spherically focused transducer on a silicone-oil droplet. The incident beam is generated considering the parameters of a typical biomedical focused transducer with an F-number of 1.6 and a driving frequency of 3.1 MHz. Using closed-form expressions of the BSCs with respect to the beam focal point [30], the radiation force is computed along the beam's axis and on the transducer's focal plane. Both Rayleigh and resonant scattering regimes are considered in this analysis. The results obtained for the Rayleigh regime are compared to those computed from Gorkov's theory [10]. A significant deviation from Gorkov's theory is noted in the axial radiation force when ultrasound absorption inside the droplet is taken into account. In addition, transverse trapping is achieved in both Rayleigh and resonant scattering regimes. Nevertheless, simultaneous axial and transverse trapping only occurs for droplets in the Rayleigh scattering regime.

II. PHYSICAL MODEL

Consider an acoustic beam of arbitrary wavefront with angular frequency ω that propagates in an inviscid infinite fluid. The fluid has ambient density ρ_0 and speed of sound c_0 . The acoustic beam is described by the excess of pressure p as a function of the position vector \mathbf{r} , with respect to a defined coordinate system. The time-dependence $e^{-i\omega t}$ is suppressed for the sake of simplicity. An spherical scatterer with radius a , density ρ_1 , and speed of sound c_1 is placed in the beam path.

A. Scattering problem

A spherically focused transducer with diameter $2b$ and curvature radius z_0 is used to produce a focused beam

(see Fig. 1) The origin of the coordinate system O is set at the transducer's focus. When the center of the sphere coincides with O , the scattering of the incident beam is referred to as the on-focus scattering configuration [30].

In the on-focus scattering formalism, the normalized amplitude of the incident pressure beam can be described in spherical coordinates $\mathbf{r} = r\mathbf{e}_r(\theta, \varphi)$, where \mathbf{e}_r is the radial unit-vector, θ and φ are the polar and the azimuthal angles, respectively. The incident pressure partial-wave expansion is given by [31]

$$p_i = \sum_{n,m} a_n^m j_n(kr) Y_n^m(\theta, \varphi), \quad (1)$$

where $\sum_{n,m} = \sum_{n=0}^{\infty} \sum_{m=-n}^n$, a_n^m are the BSCs to be determined, $k = \omega/c_0$, j_n is the n th-order spherical Bessel function, and Y_n^m is the spherical harmonic function of n th-order and m th-degree. Note that the amplitude is normalized to the pressure magnitude p_0 . Using the orthogonality properties of the spherical harmonics, the BSCs are obtained from (1) as

$$a_n^m = \frac{1}{j_n(kR)} \int_{\Omega} p_i(kR, \theta, \varphi) Y_n^{m*}(\theta, \varphi) d\Omega, \quad (2)$$

where R is the radius of a virtual spherical region where the beam propagates, $d\Omega$ is the differential solid angle, and $\Omega = \{(\theta, \varphi) : 0 \leq \theta \leq \pi, 0 \leq \varphi \leq 2\pi\}$.

Suppose now that the sphere is translated to a new point denoted by a vector \mathbf{d} as shown in Fig. 1. This corresponds to the off-focus scattering by the sphere. In spherical coordinates, the translational vector \mathbf{d} is represented with respect to the system O by (d, θ_d, φ_d) . The sphere's center defines a new coordinate system denoted by O' . The incident beam can be described in a new spherical coordinate system (r', θ', φ') as

$$\hat{p}_i = \sum_{\nu, \mu} a_{\nu}^{\mu'} j_{\nu}(kr') Y_{\nu}^{\mu}(\theta', \varphi'), \quad (3)$$

where $a_{\nu}^{\mu'}$ are called the translational BSCs. A similar expression to (2) can be obtained for the translational BSCs by using the orthogonal property of the spherical harmonics.

The relation between the position vectors of the O and O' coordinate systems is $\mathbf{r} = \mathbf{r}' + \mathbf{d}$. The translational addition theorem between the wave functions in the systems O and O' states that [28]

$$j_n(kr) Y_n^m(\theta, \varphi) = \sum_{\nu, \mu} S_{n\nu}^{m\mu}(k\mathbf{d}) j_{\nu}(kr') Y_{\nu}^{\mu}(\theta', \varphi'), \quad (4)$$

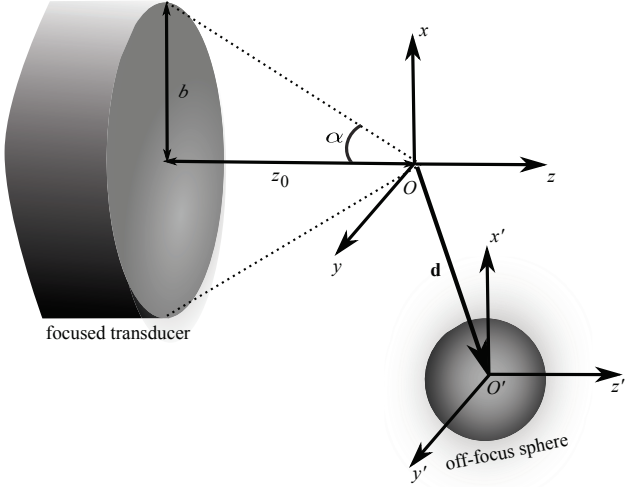


Fig. 1. Sketch of the acoustic scattering by a sphere placed anywhere in the host medium. The systems O and O' correspond to the on- and off-focus scattering configurations.

where the separation matrix is given by

$$S_{\nu n}^{\mu m}(k\mathbf{d}) = 4\pi(-1)^m \sum_{q=|n-\nu|}^{n+\nu} i^{q+n-\nu} \mathcal{G}(\nu, \mu; n, -m; q) \times j_q(kd) Y_q^{\mu-m}(\theta_d, \varphi_d), \quad (5)$$

with \mathcal{G} being the Gaunt coefficient [28]. This coefficient is zero if any of the following conditions happens $n + \nu + q$ is odd, $q > \nu + n$, or $q < |n - \nu|$.

Now, substituting (4) into (1) and use the result in (2) one obtains the translational BSCs as

$$a_{\nu}^{\mu'} = \sum_{n,m} a_n^m S_{\nu n}^{\mu m}(k\mathbf{d}), \quad (6)$$

where $\nu = 0, 1, \dots, \infty$ and $-\nu \leq \mu \leq \nu$. Note that each translational BSC is a combination of all possible BSC with respect to the system O .

Now, the scattered pressure is considered. Assume that the sphere is located at the transducer's focus (i.e. on-focus scattering configuration). The amplitude of the scattered pressure is described by the following expansion [31]

$$p_s = \sum_{n,m} s_n^m h_n^{(1)}(kr) Y_n^m(\theta, \varphi), \quad (7)$$

where s_n^m is the scattering coefficient, $h_n^{(1)}$ is the n th-order spherical Hankel function of first type. Considering a compressional sphere, the scattering coefficient is determined from the continuity condition for the pressure and the particle velocity across the sphere's surface. Further details are provided in Ref. [32]. Thus, using

the aforementioned boundary conditions, one obtains

$$s_n^m = s_n a_n^m, \quad (8)$$

where

$$s_n = -\det \begin{bmatrix} \gamma j_n(ka) & j_n(k_1 a) \\ j_n'(ka) & j_n'(k_1 a) \end{bmatrix} \times \det \begin{bmatrix} \gamma h_n^{(1)}(ka) & j_n(k_1 a) \\ h_n^{(1)'}(ka) & j_n'(k_1 a) \end{bmatrix}^{-1}, \quad (9)$$

with $\gamma = \rho_0 k_1 / (\rho_1 k)$. The prime symbol indicates differentiation with respect to the argument. According to (8) the scattering coefficient depends on the BSCs with respect to the system O and on the sphere's mechanical parameters s_n , which is independent of the choice of the coordinate system. Therefore, in the system O' the scattering coefficient becomes

$$s_n^{m'} = s_n a_n^{m'}. \quad (10)$$

Ultrasound absorption inside the sphere is considered by adding an imaginary part to the wavenumber as follows [33]

$$k_1 = \frac{\omega}{c_1} + i\alpha_0, \quad (11)$$

where α_0 is the absorption coefficient. It is remarked that shear wave propagation inside the sphere is neglected.

B. Beam-shape coefficients of a focused beam

The amplitude of the pressure generated by a transducer is given in terms of the Rayleigh integral by [34]

$$p_i = -\frac{ik\rho_0 c_0 v_0}{2\pi} \int_S \frac{e^{ik|\mathbf{r}-\mathbf{r}'|}}{|\mathbf{r}-\mathbf{r}'|} dS', \quad (12)$$

where S is the surface of the transducer's active element and v_0 is the uniform velocity distribution on S . Physically, the Rayleigh integral expresses the Huygens' principle in which the pressure at a position \mathbf{r} is the sum of wavelets generated on the surface S . Hereafter, the pressure amplitude is normalized to $p_0 = \rho_0 c_0 v_0$.

To derive the on-focus BSCs, the origin of the coordinate system is centered at the transducer focal point. By assuming that $r \ll z_0$, with $\|\mathbf{r}'\| = z_0$, the following expansion is used [35]

$$\frac{e^{ik|\mathbf{r}-\mathbf{r}'|}}{|\mathbf{r}-\mathbf{r}'|} = 4\pi \frac{e^{ikz_0}}{z_0} \sum_{n,m} (-i)^n j_n(kr) \times Y_n^m(\theta', \varphi') Y_n^{m*}(\theta, \varphi) \quad (13)$$

into (12). Thus, integrating in the angular variables

(θ', φ') yields

$$p_i = -ikz_0 e^{ikz_0} \sum_{n=0}^{\infty} i^n \sqrt{\frac{4\pi}{2n+1}} \\ \times [P_{n+1}(\cos \alpha) - P_{n-1}(\cos \alpha)] j_n(kr) Y_n^0(\theta, \varphi), \quad (14)$$

where $\alpha = \sin^{-1}(b/r_0)$ is the half-spread angle of the transducer and P_n is the Legendre polynomial of order n . The on-focus BSCs are found by comparing Eqs. (1) and (14). Accordingly,

$$a_n^m = -i^{(n+1)} k z_0 e^{ikz_0} \sqrt{\frac{4\pi}{2n+1}} \\ \times [P_{n+1}(\cos \alpha) - P_{n-1}(\cos \alpha)] \delta_{m,0}. \quad (15)$$

The partial-wave expansion of the focused beam can be compared to results based on the paraxial approximation in (12). In adopting this approximation, it is assumed that $b^2 \ll z_0^2$. Let the radial distance in cylindrical coordinates be given by $\varrho = \sqrt{x^2 + y^2}$. The pressure produced by the transducer in the focal plane is given by [36]

$$p_i(\varrho, 0) = i \left(\frac{b}{\varrho} \right) \exp \left[ik \left(\frac{\varrho^2}{z_0} + z_0 \right) \right] J_1(k\varrho \sin \alpha), \quad (16)$$

where J_1 is the first-order Bessel function. Along the transducer's axis, we have

$$p_i(0, z) = \frac{iz_0}{z - z_0} \left\{ 1 - \exp \left[\frac{ikb^2}{2} \left(\frac{1}{z} - \frac{1}{z_0} \right) \right] \right\}. \quad (17)$$

These equations will be compared to the result obtained by the partial-wave expansion given in (14).

III. ACOUSTIC RADIATION FORCE

After calculating both the incident and scattered acoustic fields through the partial-wave expansion method, the radiation force can be calculated by integrating the radiation stress tensor \mathbf{S} over the scatterer's surface. In second-order approximation, the time-averaged radiation stress tensor is given by [9]

$$\mathbf{S} = \rho_0 \overline{\mathbf{v}\mathbf{v}} - \left(\frac{\rho_0 \overline{v^2}}{2} - \frac{\overline{p^2}}{2\rho_0 c_0^2} \right) \mathbf{I}, \quad (18)$$

where the overbar denotes time-average, $\rho_0 \mathbf{v}\mathbf{v}$ is the Reynolds' stress tensor, $v = \|\mathbf{v}\|$, and \mathbf{I} is the 3×3 -unit matrix. Considering a nonviscous fluid, the radiation stress tensor is a zero divergent quantity, i.e. $\nabla \cdot \mathbf{S} = 0$. Thus, by using the Gauss divergence theorem one can show that the radiation force is given by integrating the radiation stress tensor on a control spherical surface centered at the target object. Furthermore, the radius of

the control surface r lies in the farfield, i.e. $kr \gg 1$. Therefore, the radiation force is given by

$$\mathbf{f} = -r^2 \int_{\Omega} \mathbf{S} \cdot \mathbf{e}_r d\Omega, \quad kr \gg 1. \quad (19)$$

One can show that the Cartesian components of the radiation force can be expressed as [22], [?]

$$\mathbf{f} = \pi a^2 E_0 (Y_x \mathbf{e}_x + Y_y \mathbf{e}_y + Y_z \mathbf{e}_z), \quad (20)$$

where $E_0 = p_0^2 / (2\rho_0 c_0^2)$ is the characteristic energy density of the incident wave, and \mathbf{e}_x , \mathbf{e}_y and \mathbf{e}_z are the Cartesian unit-vectors. The radiation force functions are given by

$$Y_x + iY_y = \frac{i}{2\pi(ka)^2} \sum_{n,m} \sqrt{\frac{(n+m+1)(n+m+2)}{(2n+1)(2n+3)}} \\ \times (S_n a_n^m a_{n+1}^{m+1*} + S_n^* a_n^{-m*} a_{n+1}^{-m-1}), \quad (21)$$

$$Y_z = \frac{1}{\pi(ka)^2} \text{Im} \sum_{n,m} \sqrt{\frac{(n-m+1)(n+m+1)}{(2n+1)(2n+3)}} \\ \times S_n a_n^m a_{n+1}^{m*}, \quad (22)$$

where 'Im' denotes the imaginary part, the symbol * means complex conjugation, and

$$S_n = s_n + s_{n+1}^* + 2s_n s_{n+1}^*. \quad (23)$$

It is worth to note that the radiation force functions Y_x , Y_y , and Y_z are real-valued quantities.

IV. RESULTS AND DISCUSSION

Consider an acoustic beam that is generated in water for which $c_0 = 1500$ m/s and $\rho_0 = 1000$ kg/m³. The focused transducer has a radius $b = 22$ mm, a F-number of 1.6, and operates at 3.1 MHz. Note that $(b/z_0)^2 = 0.1$, which ensures the paraxial approximation for the incident beam. The magnitude of the pressure generated by the transducer is $p_0 = \rho_0 c_0 v_0 = 10^5$ Pa. A droplet made out of silicone-oil ($c_1 = 974$ m/s, $\rho_1 = 1004$ kg/m³, and $\alpha_0 = 21$ Np/m at 3.1 MHz) is used as the target object.

The truncation error in computing the translational BSCs in (6) is analyzed in Appendix A. Accordingly, the truncation order for the index n necessary to achieve a certain error ϵ is given by

$$N = \nu + kd + 1.8(\log \epsilon^{-1})^{2/3} (kd)^{1/3}. \quad (24)$$

The error considered in the translational BSC computations is $\epsilon = 10^{-6}$. The truncation order L of the radiation force series in (22) is established by the scattering coefficient ratio $|s_L^m / s_0^0| < 10^{-7}$.

In Fig. 2, the pressure amplitude (normalized to p_0) produced by the focused transducer is shown along both

x and z directions. The pressure is computed using the partial-wave expansion method and the paraxial approximation based on (16). Good agreement is found between the methods in the transverse direction and in the vicinity of the focal region. Though moving away from the focal region, the partial-wave expansion method deviates from the paraxial approximation result. This happens because the partial-wave expansion is valid in the vicinity of the focal region, i.e. $r \ll z_0$.

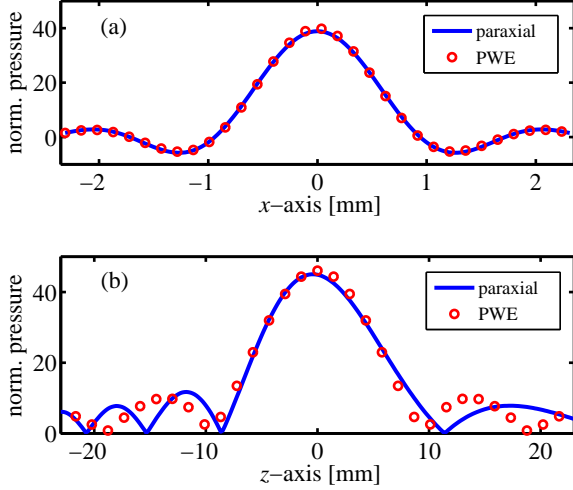


Fig. 2. Pressure amplitude generated by the spherically focused transducer with aperture 44 mm and F-number of 1.6, operating at 3.1 MHz. The pressure is evaluated along (a) the transverse and (b) the axial directions using the partial-wave expansion (PWE) method and the paraxial approximation.

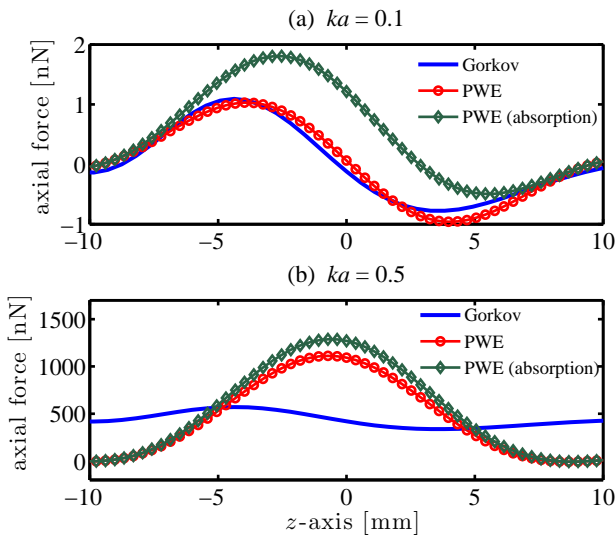


Fig. 3. Axial radiation force versus the droplet's position along z direction in the focal plane. The force is computed through the partial-wave expansion (PWE) and Gorkov's methods. The size factors of the sphere are (a) $ka = 0.1$ and (b) $ka = 0.5$.

Figure 3 exhibits the axial radiation force versus the droplet's position along the transducer's axis (z direction). The droplet's size factors are $ka = 0.1$ (Rayleigh regime) and $ka = 0.5$ (resonant regime). The solid line represents the radiation force computed with Gorkov's method. Good agreement between the methods is found when no ultrasound absorption is considered in the droplet. However, when ultrasound absorption is taking into account, a significant deviation between these methods is observed. This result is expected since the acoustic radiation force caused by a plane traveling wave on a sphere depends on the sum of the scattered and absorbed power [9]. The Gorkov's theory does not take into account absorption inside the particle. Therefore, if absorption is considered, the radiation force will be larger than in the case where absorption is neglected [37], [38]. The droplet with $ka = 0.1$ is axially trapped along the transducer axis at $z = 2.5$ mm (with absorption). Note that a nonabsorptive droplet would be trapped at $z = 0$. Gorkov's method no longer describes the behavior of the radiation force generated by the focused transducer when $ka = 0.5$. Furthermore, it is not possible to axially trap the droplet with the analyzed transducer at this size factor. This can be understood as follows. The radiation force exerted on a small particle by the spherically focused beam is formed by two contributions [10]: "the scattering force" caused mostly by the traveling wave part of the beam, while "the gradient force" is due to the spatial variation of the potential and kinetic energy densities of the beam. As the size factor increases, so does the scattering force. When this force overcomes the gradient force, the axial trapping is no longer possible. This might be prevented using tightly focused beams [5].

The transverse radiation force versus the droplet's position along x direction in the focal plane is shown in Fig. 4. Excellent agreement is found between the partial-wave expansion and Gorkov's methods when $ka = 0.1$. Some deviation between the methods arises when $ka = 0.5$. Note that the results with and without absorption are very alike. The transverse trapping happens for both $ka = 0.1$ and 0.5 , because no scattering radiation force is present in the transverse direction. Only the gradient radiation force appears in this direction. Based on Figs. 3 and 4 we conclude that the focused transducer forms a 3D acoustical tweezer for silicone-oil droplets in the Rayleigh scattering regime.

The axial radiation force versus the droplet's position along z direction for the resonant scattering regime ($ka = 1$ and 5) is shown in Fig. 5. In this case, the scattering force totally overcomes the gradient force. Thereby, no trapping is possible in the axial direction with the analyzed transducer. The axial radiation force

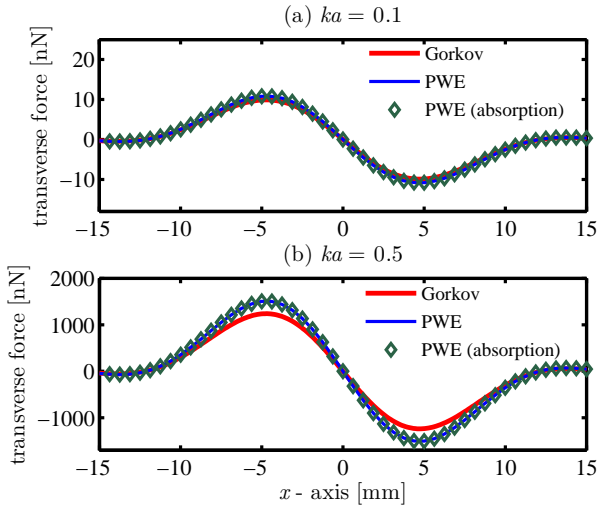


Fig. 4. Transverse radiation force versus the droplet's position along x direction in the focal plane. The force is computed through the partial-wave expansion and Gorkov's methods. The size factors are (a) $ka = 0.1$ and (b) $ka = 0.5$.

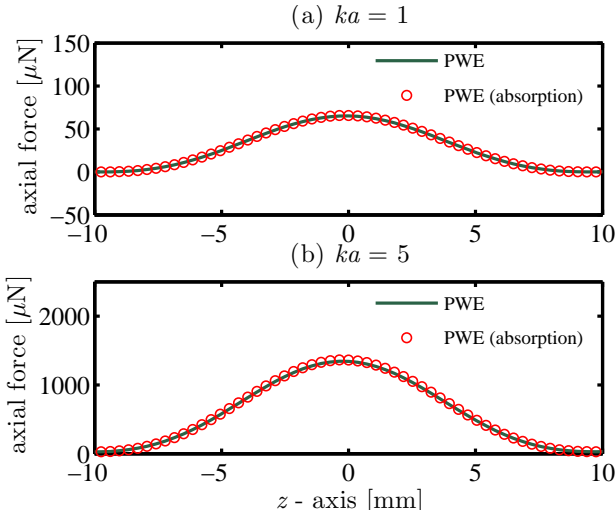


Fig. 5. Axial radiation force versus the droplet's position along z direction for the resonant scattering regime (a) $ka = 1$ and (b) $ka = 5$.

pushes the droplet to the forward scattering direction.

In Fig. 6, the transverse radiation force versus the droplet's position along x direction is displayed for the resonant scattering regime ($ka = 1$ and 5). It is clearly shown that the transverse trapping is still possible in this scattering regime. This happens because the incident beam is tightly focused in the transverse direction. Moreover, the transverse radiation force remains practically the same regardless of ultrasound absorption within the droplet.

The vector field of the transverse radiation force on the silicone-oil droplet placed in the transducer focal plane is displayed in Fig. 7. The background map represents the

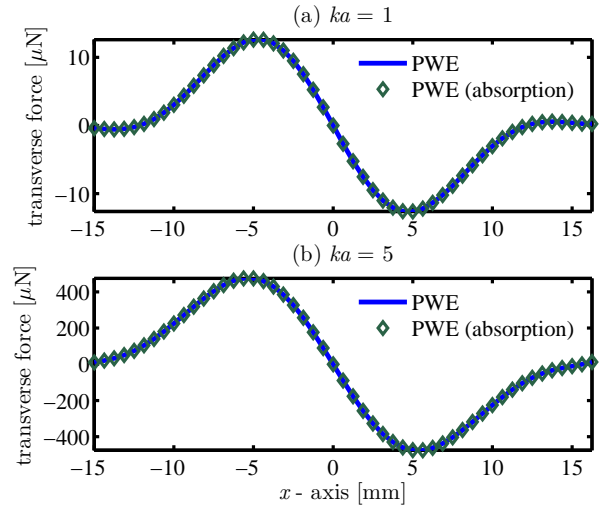


Fig. 6. Transverse radiation force on a silicone oil droplet (with and without attenuation) in the resonant scattering regime (a) $ka = 1$ and (b) $ka = 5$.

axial radiation force exerted on the droplet. If the droplet lies in the circular region with radius of 0.5 mm around the focus point, it will be attracted and trapped along the transducer's axis. The droplet is transversely trapped by a force of about $10 \mu\text{N}$ (see Fig. 4), but it will be further pushed axially by a force of $60 \mu\text{N}$. Therefore, the focused transducer operates as a 2D acoustical tweezer for droplets in the resonant scattering regime ($ka = 1$).

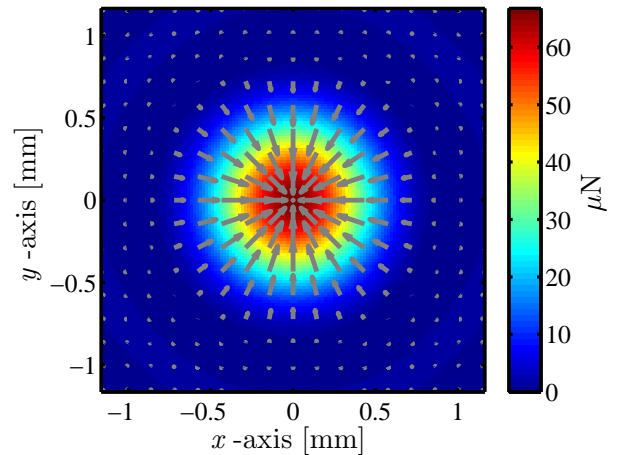


Fig. 7. Vector field of the radiation force in the transducer focal plane produced on the silicone oil droplet in the resonant regime $ka = 1$. The vector field is plot on top of the axial radiation force.

V. SUMMARY AND CONCLUSIONS

A method to compute the axial and the transverse acoustic radiation force on a sphere based on the translational addition theorem for spherical wave functions was

presented. The method relies on the fact that once the BSCs are known with respect to a coordinate system, they can be calculated in a new translated coordinate system. The radiation force generated by an ultrasound focused beam in the paraxial approximation and exerted on a silicone-oil droplet placed anywhere in the host medium was calculated using the proposed method. Both axial and transverse radiation forces were computed in the Rayleigh and resonant scattering regimes. In the Rayleigh regime, the obtained results were compared to Gorkov's radiation force theory. Good agreement was found between these methods when ultrasound absorption inside the droplet was neglected. Nevertheless, a significant deviation between the results takes place in the axial radiation force when the ultrasound absorption is considered. It was shown that the transducer under investigation, with driving frequency of 3.1 MHz and an F-number of 1.6, can operate as a single-beam acoustical tweezer in 3D for the Rayleigh scattering regime. In contrast, only transverse trapping of the silicone-oil droplet was achieved for the resonant scattering regime.

In conclusion, the translational addition theorem of spherical wave functions was used in combination with the partial-wave expansion to compute the axial and the transverse acoustic radiation force on a sphere. This method may become a useful tool in the design and evaluation of acoustical tweezers in particle manipulation applications.

ACKNOWLEDGEMENTS

This work was supported by grants CAPES 2163/2009-AUX-PE-PNPD, CNPq 306697/2010-6, and CNPq 481284/2012-5 (Brazilian agencies).

APPENDIX

Assume the series in (6) is truncated in $n = N$. Thus, the truncation error is given by

$$\epsilon = \left| \sum_{n=N+1}^{\infty} \sum_{m=-n}^n a_n^m S_{\nu n}^{\mu m}(k\mathbf{d}) \right|. \quad (25)$$

We consider the truncation error for a plane progressive wave. This analysis is the upper limit case for the error because the normalized pressure amplitude of an acoustic beam is smaller than that of a normalized plane wave. The BSC of a plane wave described by $\hat{p} = e^{ikz}$ is $a_n^m = i^n \sqrt{4\pi(2n+1)}\delta_{m,0}$. Substituting this into (25) yields

$$\epsilon = \sqrt{4\pi} \left| \sum_{n=N+1}^{\infty} i^n \sqrt{2n+1} S_{\nu, n}^{\mu, 0}(k\mathbf{d}) \right|. \quad (26)$$

The leading term of the separation matrix in (5) is related to the spherical Bessel function of smallest order, i.e. $q = |n - \nu|$. Therefore, the truncation error can be approximated to

$$\epsilon \simeq (4\pi)^{3/2} \sqrt{2N - 2\nu + 3} \left| \mathcal{G}(\nu, \mu; N + 1, 0; N - \nu + 1) \times j_{N-\nu+1}(kd) Y_{N-\nu+1}^{\mu}(\theta_d, \varphi_d) \right|. \quad (27)$$

After integrating over (θ_d, φ_d) , we obtain

$$\epsilon \simeq |j_{N-\nu+1}(kd)|. \quad (28)$$

When the order of the spherical Bessel function is larger than its argument, the error can be approximated to [39]

$$\epsilon \simeq \left| \frac{1}{2} \sqrt{\frac{1}{xf(x, L)}} \exp \left[f(x, L) - \left(L + \frac{3}{2} \right) \ln \left(L + \frac{3}{2} + \frac{f(x, L)}{x} \right) \right] \right|, \quad (29)$$

where $L = N - \nu + 1$, $x = kd$, and $f(x, L) = \sqrt{(L + 3/2)^2 - x^2}$. We define $L + 3/2 = x(1 + \delta)$. Since the spherical Bessel function decreases rapidly as the order becomes larger than the argument, the parameter δ is assumed to be much smaller than the unit. Therefore, the error can be expressed as

$$\epsilon \simeq (2\delta)^{-1/4} e^{-x(2\delta)^{3/2}/3} \quad (30)$$

The second term in this equation is much smaller than the first and then dominates the error. Thus, taking the logarithm on both sides of this equation, we can estimate the truncation order in (6) as

$$N = \nu + kd + 1.8(\log \epsilon^{-1})^{2/3} (kd)^{1/3}. \quad (31)$$

The term $\log \epsilon^{-1}$ is closely related to the number of precision digits, which is given by the nearest integer to $(\log \epsilon^{-1} + 1.0 - \log 2)$.

REFERENCES

- [1] J. Wu, "Acoustical tweezers," *J. Acoust. Soc. Am.*, vol. 89, pp. 2140–2143, 1991.
- [2] A. Lenshof, C. Magnusson, and T. Laurell, "Acoustofluidics 8: Applications of acoustophoresis in continuous flow microsystems," *Lab-on-a-Chip*, vol. 12, pp. 1210–1223, 2012.
- [3] J. Shi, D. Ahmed, X. Mao, S. Lin, A. Lawit, and T. Huang, "Acoustic tweezers: patterning cells and microparticles using standing surface acoustic waves (SSAW)," *Lab on a Chip*, vol. 9, pp. 2890–2895, 2009.
- [4] C. R. P. Courtney, C.-K. Ong, B. W. Drinkwater, and P. D. Wilcox, "Manipulation of microparticles using phase-controllable ultrasonic standing waves (EL)," *J. Acoust. Soc. Am.*, vol. 128, pp. 195–199, 2010.
- [5] J. Lee, S. Teh, A. Lee, H. Kim, C. Lee, and K. Shung, "Single beam acoustic trapping," *Appl. Phys. Lett.*, vol. 95, p. 073701, 2009.

- [6] L. V. King, "On the acoustic radiation pressure on spheres," *Proc. R. Soc. A*, vol. 147, no. 861, pp. 212–240, 1934.
- [7] T. F. W. Embleton, "Mean force on a sphere in a spherical sound field. I. (Theoretical)," *J. Acoust. Soc. Am.*, vol. 26, pp. 40–45, 1954.
- [8] K. Yosioka and Y. Kawasima, "Acoustic radiation pressure on a compressible sphere," *Acustica*, vol. 5, pp. 167–173, 1955.
- [9] P. J. Westervelt, "Acoustic radiation pressure," *J. Acoust. Soc. Am.*, vol. 29, pp. 26–29, 1957.
- [10] L. P. Gorkov, "On the forces acting on a small particle in an acoustic field in an ideal fluid," *Sov. Phys. Dokl.*, vol. 6, pp. 773–775, 1962.
- [11] W. L. Nyborg, "Radiation pressure on a small rigid sphere," *J. Acoust. Soc. Am.*, vol. 42, pp. 947–952, 1967.
- [12] T. Hasegawa and K. Yosioka, "Acoustic-radiation force on a solid elastic sphere," *J. Acoust. Soc. Am.*, vol. 46, pp. 1139–1143, 1969.
- [13] T. Hasegawa, T. Kido, S. Takeda, N. Inoue, and K. Matsuzawa, "Acoustic radiation force on a rigid sphere in the near field of a circular piston vibrator," *J. Acoust. Soc. Am.*, vol. 88, no. 3, pp. 1578–1583, 1990.
- [14] F. G. Mitri, "Near-field single tractor-beam acoustical tweezers," *Appl. Phys. Lett.*, vol. 103, no. 11, p. 114102, 2013.
- [15] X. Chen and R. Apfel, "Radiation force on a spherical object in an axisymmetric wave field and its application to the calibration of high-frequency transducers," *J. Acoust. Soc. Am.*, vol. 99, pp. 713–724, 1996.
- [16] P. L. Marston, "Axial radiation force of a Bessel beam on a sphere and direction reversal of the force," *J. Acoust. Soc. Am.*, vol. 120, pp. 3518–3524, 2006.
- [17] F. G. Mitri, "Acoustic scattering of a high-order Bessel beam by an elastic sphere," *Ann. Phys.*, vol. 323, pp. 2840–2850, 2008.
- [18] —, "Langevin acoustic radiation force of a high-order Bessel beam on a rigid sphere," *IEEE Trans. Ultrason. Ferroelec. Freq. Contr.*, vol. 56, pp. 1059–1064, 2009.
- [19] M. Azarpeyvand, "Acoustic radiation force of a Bessel beam on a porous sphere," *J. Acoust. Soc. Am.*, vol. 131, pp. 4337–4348, 2012.
- [20] X. Zhang and G. Zhang, "Acoustic radiation force of a gaussian beam incident on spherical particles in water," *Ultras. Med. Biol.*, vol. 38, pp. 2007–2017, 2012.
- [21] J. Lee and K. K. Shung, "Radiation forces exerted on arbitrarily located sphere by acoustic tweezer," *J. Acoust. Soc. Amer.*, vol. 120, pp. 1084–1094, 2006.
- [22] G. T. Silva, "An expression for the radiation force exerted by an acoustic beam with arbitrary wavefront," *J. Acoust. Soc. Am.*, vol. 130, pp. 3541–3545, 2011.
- [23] —, "Off-axis scattering of an ultrasound Bessel beam by a sphere," *IEEE Trans. Ultrason. Ferroelec. Freq. Contr.*, vol. 58, pp. 298–304, 2011.
- [24] F. G. Mitri and G. T. Silva, "Off-axial acoustic scattering of a high-order Bessel vortex beam by a rigid sphere," *Wave Motion*, vol. 48, pp. 392–400, 2011.
- [25] G. T. Silva, T. P. Lobo, and F. G. Mitri, "Radiation torque produced by an arbitrary acoustic wave," *Europhys. Phys. Lett.*, vol. 97, p. 54003, 2012.
- [26] G. T. Silva, J. H. Lopes, and F. G. Mitri, "Off-axial acoustic radiation force of repulsor and tractor Bessel beams on a sphere," *IEEE Trans. Ultrason. Ferroel. Freq. Control*, vol. 60, pp. 1207–1212, 2012.
- [27] G. Gouesbet, C. Letellier, K. F. Ren, and G. Gréhan, "Discussion of two quadrature methods of evaluating beam-shape coefficients in generalized Lorenz-Mie theory," *Appl. Opt.*, vol. 35, pp. 1537–1542, 1996. *Applied Optics*, Vol. 35, Issue 9, pp. 1537-1542 (1996)
- [28] P. A. Martin, *Multiple Scattering Interaction of Time-Harmonic Waves with N Obstacles*. Cambridge, UK: Cambridge University Press, 2006, ch. 3.
- [29] O. Moine and B. Stout, "Optical force calculations in arbitrary beams by use of the vector addition theorem," *J. Opt. Soc. Am. B*, vol. 22, pp. 1620–1631, 2005.
- [30] P. L. Edwards and J. Jarzynski, "Scattering of focused ultrasound by spherical microparticles," *J. Acoust. Soc. Am.*, vol. 74, pp. 1006–1012, 1983.
- [31] E. G. Williams, *Fourier Acoustics: Sound Radiation and Nearfield Acoustical Holography*. San Diego, CA: Academic Press, Inc., 1999, ch. 6.
- [32] V. C. Anderson, "Sound scattering from a fluid sphere," *J. Acoust. Soc. Am.*, vol. 22, pp. 426–431, 1950.
- [33] T. L. Szabo, "Time domain wave equations for lossy media obeying a frequency power law," *J. Acoust. Soc. Am.*, vol. 96, pp. 491–500, 1994.
- [34] A. D. Pierce, *Acoustics: An Introduction to Its Physical Principles and Applications*. Melville, NY: Acoustical Society of America, 1989, p. 215.
- [35] D. Colton and R. Kress, *Inverse Acoustic and Electromagnetic Scattering Theory*. Berlin, Germany: Springer-Verlag, 1998, eq. 2.42.
- [36] B. G. Lucas and T. G. Muir, "The field of a focusing source," *J. Acoust. Soc. Am.*, vol. 72, pp. 1289–1289, 1982.
- [37] R. Löfstedt and S. Putterman, "Theory of long wavelength acoustic radiation pressure," *J. Acoust. Soc. Am.*, vol. 90, no. 4, pp. 2027–2033, 1991.
- [38] G. T. Silva, "Acoustic radiation force and torque on an absorbing compressible particle in an inviscid fluid," *Pre-print*, 2014, arXiv:1307.4705v2 [physics.class-ph].
- [39] J. Song and W. C. Chew, "Error analysis for the truncation of multipole expansion of vector Green's functions," *IEEE Micro. Wireless Comp. Lett.*, vol. 11, pp. 311–313, 2001.